CHEMISTRY
A EUROPEAN JOURNAL

VIP

The First Studies of a Tetrathiafulvalene-σ-Acceptor Molecular Rectifier

Gregory Ho,[a] James R. Heath,*[a, b] Mykola Kondratenko,[c] Dmitrii F. Perepichka,*[c, d] Karin Arseneault,[e] Michel Pézolet,[e] and Martin R. Bryce[f]

Abstract: Langmuir–Blodgett monolayers of a donor–acceptor diad TTF-σ-(trinitrofluorene) (**8**) with an extremely low HOMO–LUMO gap (0.3 eV) have been used to create molecular junction devices that show rectification behavior. By virtue of structural similarities and position of molecular orbitals, **8** is the closest well-studied analogue of the model Aviram–Ratner unimolecular rectifier (TTF-σ-TCNQ). Compressing the monolayer results in aligning the molecules, and is followed by a drastic increase in the rectification ratio. The direction of rectification depends on the electrodes used and is different in n-Si/**8**/Ti and Au/**8**/$C_{16}H_{33}S$-Hg junctions. The molecular nature of such behavior was corroborated by control experiments with fatty acids and by reversing the rectification direction with changing the molecular orientation (Au/D-σ-A versus Au/A-σ-D).

Keywords: donor–acceptor systems · HOMO–LUMO gap · molecular devices · rectifiers · tetrathiafulvalene

Introduction

Shortly after the 1973 discovery of metallic conductivity in the purely organic donor–acceptor (D–A) complex of tetrathiafulvalene (TTF) and tetracyanoquinodimethane (TCNQ),[1] Aviram and Ratner proposed the concept of a molecular rectifier.[2] They postulated that a covalent donor-bridge-acceptor (D-σ-A) molecule, such as TTF-σ-TCNQ (**1**; in which σ is a saturated aliphatic linker), when placed between two electrodes can act as a rectifier that preferably passes the current in one direction. At the appropriate voltage, the electron and hole injection from the Fermi levels of the electrodes into the molecular LUMO and HOMO levels results in charge-separated species $TTF^{\bullet+}$-σ-$TCNQ^{\bullet-}$, which annihilate by inelastic electron tunneling through the σ-linker, allowing current (electron) flow in the acceptor–donor direction. Under this mechanism, the reverse electron flow would require a much higher voltage to fit the larger gap between the low-energy local HOMO orbital of the acceptor moiety and the higher energy local LUMO orbital of the donor moiety.

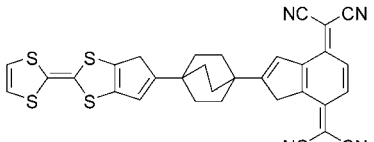

TTF–σ–TCNQ, **1**

[a] G. Ho, Prof. J. R. Heath
Department of Chemistry and Biochemistry
University of California, Los Angeles, CA 90095 (USA)
E-mail: heath@caltech.edu

[b] Prof. J. R. Heath
Department of Chemistry
Caltech MC 127–72, Pasadena, CA 91125 (USA)
Fax: (+1) 310-206-4038

[c] M. Kondratenko, Prof. D. F. Perepichka
INRS-Énergie, Matériaux et Télécommunications
Université du Québec, Varennes, J3X 1S2 (Canada)
Fax: (+1) 450-929-8102
E-mail: perepichka@emt.inrs.ca

[d] Prof. D. F. Perepichka
Institute of Physical Organic and Coal Chemistry
National Academy of Sciences of Ukraine, Donetsk 83114 (Ukraine)

[e] K. Arseneault, Prof. M. Pézolet
Département de Chimie, Université Laval
Québec, G1K 7P4 (Canada)

[f] Prof. M. R. Bryce
Department of Chemistry, University of Durham
Durham, DH1 3 LE (UK)

Supporting information for this article is available on the WWW under http://www.chemeurj.org/ or from the author. Supporting information for this article is available on the WWW under http://www.chemeurj.orgor from the author: Figure of different conformations of **8a**; RAIRS spectra of **8** in LB monolayer transferred on gold surface; plot of the rectification ratio vs applied bias for different junction devices.

DOI: 10.1002/chem.200401121

Since then, numerous experimental strategies to achieve rectification in donor–acceptor molecules have been attempted.[3–5] Various molecular structures, electrodes, and junction assembly approaches have been tested, although the precise mechanism for the rectification in molecular junctions is still a subject of controversy. A great many studies have been devoted to molecular junctions with D-π-A compounds (such as **2**–**4**, π is a conjugated bridge).[6–12] The

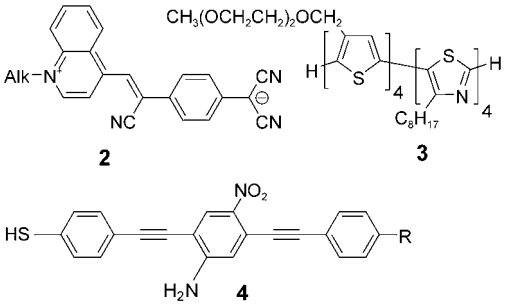

most studied among these, zwitterionic molecule **2** (and its derivatives), has been explored since 1990,[6–8] and by now the origin of the rectification in these molecules has been established, although a different rectification mechanism was proposed.[7a] Rectification behavior has also been observed in π-electron molecular systems lacking the formal D–A design,[13–17] but asymmetrically coupled to the electrodes.[18]

At the same time, very few D-σ-A molecules with a non-conjugated bridge (e.g., **5** and **6**) have been studied as molecular rectifiers.[19] Moreover, all molecular electronic devices studied experimentally to date were constructed by using relatively weak donor and acceptor fragments, resulting in a rather high (⩾0.5 eV) HOMO–LUMO gap. Recent high-level density functional theory (DFT) calculations of a D–A molecule between two gold electrodes failed to show rectification for the weak donor and acceptor moieties studied (aminophenyl and nitrophenyl, respectively), and the authors argue that molecules with a much smaller HOMO–LUMO gap are necessary to generate rectification.[20] However, there are no reported investigations of rectification behavior in molecules with very strong π-electron donor (like TTF) and π-electron acceptor (like TCNQ) moieties, presumably due to synthetic unavailability of such compounds. There are two reports on studying molecular rectification in TCNQ derivatives possessing weak electron-donor fragments;[19a,16] one of us reported studies on molecular electronic devices (switches) based on TTF supramolecular systems with a moderate electron acceptor moiety,[21] but the original Aviram–Ratner model has not as yet been experimentally tested.

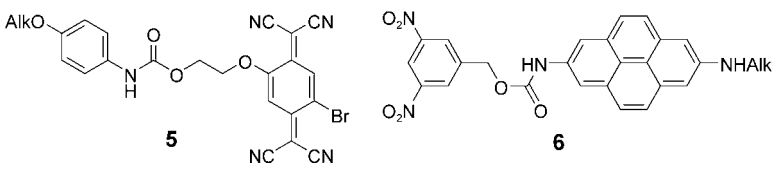

Some of us have recently reported the synthesis of TTF donor–acceptor diads (**7** and **8**) with an unprecedentedly low HOMO–LUMO gap of approximately 0.3 eV.[22] By

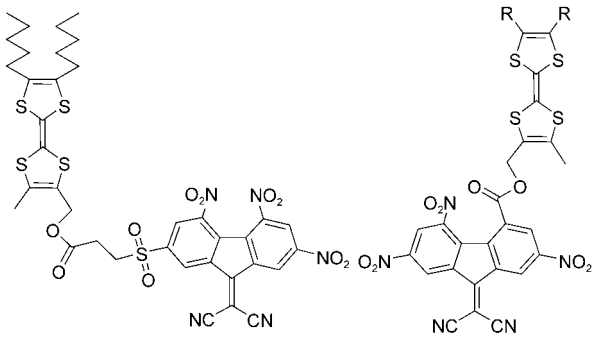

virtue of having very strong electron-donor and -acceptor components separated by a saturated bridge, and by having an amphiphilic structure enabling fabrication of a Langmuir–Blodgett (LB) type device, these molecules are suitable candidates for molecular electronic devices, particularly in the frame of the original Aviram–Ratner rectification ansatz. However, the flexible σ linker in **7** is long enough to allow an unwanted head-to-tail intramolecular-complex conformation;[22] besides, it introduces an additional tunneling resistance. This problem is eliminated in compound **8** by using a short σ linker. Here we report fabrication and studies of monolayer, tunnel junction devices with a TTF-based D-σ-A diad, in which A is a fluorene electron acceptor with an electron affinity similar to TCNQ. Two different junction setups are investigated, in combination with the effects of molecular alignment and molecular orientation. In all cases, rectification is observed; moreover, the magnitude and orientation of the rectification is found to correlate with the electrode materials, the molecular alignment, and the molecular orientation.

Results and Discussion

Geometry and electronic structure of 8: To evaluate the molecular properties of the diad **8**, we calculated the geometry and the orbital energies of a simplified molecule **8a** (lacking long alkyl substituents) by using density functional theory

(DFT) at the B3LYP level, with a 6–31G(d) basis set (Figure 1). This method is reliable for describing geometry and orbital energies of organic molecules,[23] and was recently successfully used to predict the HOMO–LUMO gap of a related low-gap TTF-σ-TCNQ diad.[24] In accordance with experimental observations,[22a] our calculations show no possibility for intramolecular π–π complexation between the TTF and fluorene fragments. The conformational analysis reveals the presence of several stable conformations, differing in energy by 1–2.5 kcal mol^{-1}. The geometry of the lowest energy conformation is given in Figure 1. The calculated structural features of **8a** are similar to those found by X-ray crystallographic analysis in the related compound **9**;[22a] this confirms the applicability of the chosen theoretical model. The variation of the calculated HOMO–LUMO gap (0.30–0.35 eV) in different conformations is low (in contrast to diads with a long σ linker[24]), and very close to the experimentally observed electrochemical gap of compound **8** (0.29 V), obtained from cyclic voltammetry experiments (Figure 1). The HOMO–LUMO gap of **8** fits almost exactly the original Aviram–Ratner model, in which the asymmetric I–V curve was calculated assuming a 0.3 eV gap.[2] At the same time, the electronic state of **8** (and, therefore, the rectification behavior) in the tunneling junction might be difficult to predict. Although the ground state of individual molecules is neutral, the electron transfer is very facile in these systems, as manifested by a relatively weak ESR signal in solution. When an LB film of **8** is sandwiched between conducting electrodes, the energy levels may be shifted significantly (due to intermolecular interactions, electrode interface effects,[25] and the applied electric field[19b]). Such shifts may even cause the gap to close, so that the zwitterionic biradical ground state of **8** in the junction is a possibility.

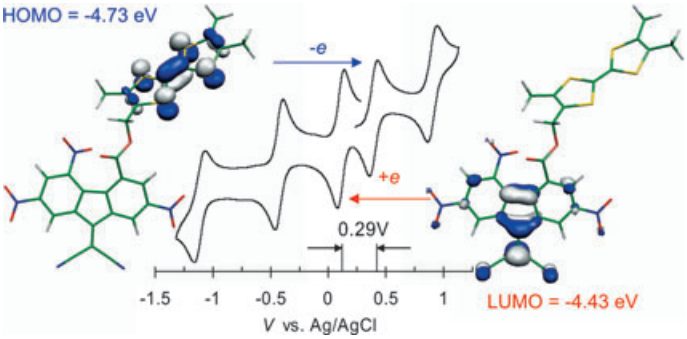

Figure 1. The calculated [B3LYP/6–31G(d)] geometry of **8a** in the minimum energy conformation and the plot of HOMO (left) and LUMO (right) orbitals. The cyclic voltammogram (middle) of compound **8** confirms the low value of the HOMO–LUMO gap.

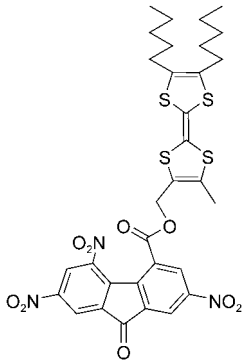

9

Preparation of LB monolayers of 8: The LB films were prepared by spreading a dilute, fresh solution of **8** in $CHCl_3$ on a water surface, and then decreasing the surface area, generating a pressure–area isotherm (Figure 2, top). Decreasing the area below about 60 Å^2 per molecule results in a sharp increase of the pressure up to a short plateau at approximately 30–35 Å^2 per molecule, at which point the monolayer collapses. The uneven shape of the isotherm giving rise to a shoulder at about 50 Å^2 per molecule may be due to the conformational flexibility of **8**, resulting in multiple molecular orientations, each with their own characteristic molecular area.

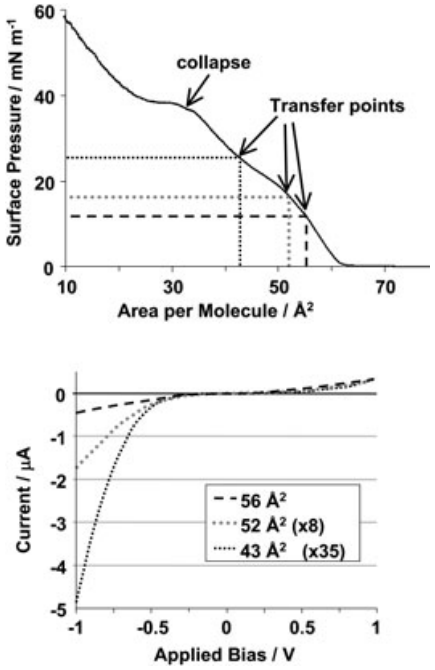

Figure 2. Top: Surface pressure isotherm of **8**. The indicated transfer pressures of the films that were used for device fabrication were 12, 16, and 25 mN m^{-1}, corresponding to 56, 52, and 43 Å^2 per molecule. Bottom: The current–voltage curves obtained from the n-Si/**8**/Ti molecular tunnel junction devices made from the three films indicated in the isotherm measurements. Note that as the area per molecule decreases, the rectification character increases (by a factor of 10), but the current decreases. Both the increased current rectification and the decrease in current magnitude are indicative of an increased alignment of the molecular monolayer.

Brewster angle microscopy (BAM) of the Langmuir monolayers revealed small spots (~100 microns in diameter) on the trough surface that appear immediately upon the dropwise addition of a solution of **8** in $CHCl_3$ to the surface (Figure 3). These presumably correspond to molecular aggregates. The spots, however, spread out within seconds to form a microscopically uniform surface. During the monolayer compression (at 2 $cm^2 min^{-1}$), the surface pressure was periodically held steady to check the stability of the films. At a fixed pressure of 12 $mN m^{-1}$, the area dropped by less than 0.4% over 2 minutes, indicating a very stable monolayer. At higher pressures of 16 and 25 $mN m^{-1}$, there was an increased rate of monolayer relaxation (the trough area dropped by 1.6 and 2.9%, respectively, over a period 2 min). This is at least consistent with the suggested conformational changes to **8** at pressures ~16–25 $mN m^{-1}$. For all films investigated here, the few small spots (presumably dust particles) captured by the BAM remained steady on the surface for the entire two minutes, indicating that the formed LB films were 2D solids. The compressed LB films were transferred onto hydrophilic (oxygen-terminated) polycrystalline n-doped silicon substrates at three values of surface pressure (Figure 2, top). The transfer direction (Si slides start out dipped into the water before the addition of the molecules, and are then lifted up through the LB film) necessarily resulted in the acceptor moiety being exposed to the Si surface (X-deposition). The more polar dicyanomethylenefluorene fragments of **8** were presumably exposed to the polar water phase, whereas the hydrophobic trialkyl-TTF moieties are stretched into the air. Indeed, a high water contact angle was observed (89°), consistent with a hydrocarbon-terminated monolayer surface.

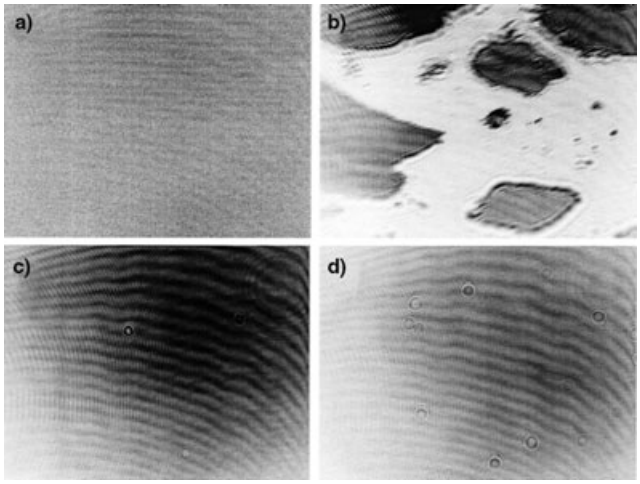

Figure 3. BAM images of a) clean Langmuir trough; b) same, immediately after dropwise addition of a solution of **8** in $CHCl_3$; c) LB film of **8** at 12 $mN m^{-1}$; d) LB film of **8** at 26 $mN m^{-1}$ (the picture width is 480 μm).

Spectroscopic characterization of LB monolayers of 8: To establish the preservation of chemical structure of **8** in transferred LB monolayers, we have performed an infrared spectroscopic characterization of films transferred (X-deposition) onto the surface of a Ge crystal (which somewhat resembles the chemical properties of Si electrodes used in junction devices) by the attenuated total reflectance (ATR) technique. We also investigated films transferred onto a gold substrate by grazing-angle reflection–absorption infrared spectroscopy (RAIRS). Comparison with the spectrum of bulk **8** (powdered in KBr, Figure 4), as well as with spectra of compounds containing separate TTF and fluorene fragments, reveals the presence of all main absorption peaks, suggesting the structural integrity of the transferred molecules (see Table 1). In spite of certain differences (such as much broader lines in the LB film and somewhat different relative intensities) expected for different molecular orientations and intermolecular interactions in the LB film and in the crystal, one can clearly see the presence of a potentially vulnerable ester group (C=O, C–O), the electron-acceptor fluorene fragment (cyano and nitro-groups as well as aromatic C=C bonds), and the electron-donor trialkyl-TTF fragment (CH_2, CH_3). The position of the significantly broadened CN band (2205 cm^{-1}, similar to that in the bulk sample) is between those for a completely neutral (2225 cm^{-1}) and radical-anion species (2180 cm^{-1}),[22a] suggesting a partial charge transfer (either from the TTF fragment or from the Ge surface). The lack of strong characteristic absorption bands of the TTF core precludes a detailed analysis of this fragment, but the absence of a sulfoxide bond (at ca. 970–990 cm^{-1}),[26] expected for S-oxidized species, suggests that no irreversible oxidative decomposition of this fragment took place (although one cannot exclude a reversible formation of a TTF radical cation).

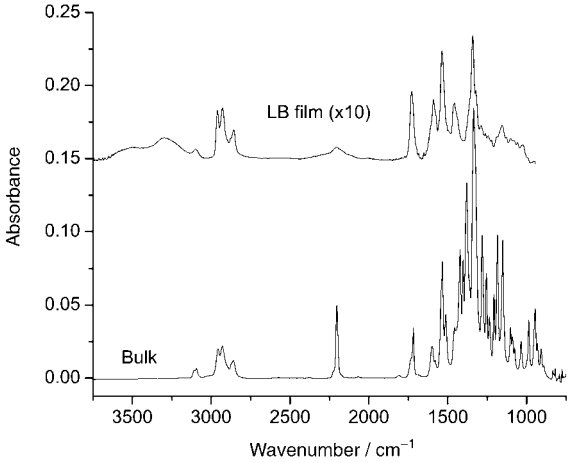

Figure 4. FTIR spectra of compound **8** in bulk (in transmission mode in KBr) and in LB monolayer (in ATR mode).

To shed more light on the structure of LB film of **8**, we performed an orientation analysis of the films transferred on a Ge crystal using polarized light. ATR spectra were thus recorded by using polarized infrared radiation, and the di-

Table 1. Assignment of the major IR absorption peaks of **8** in the LB film and in bulk, their relative intensity (I_X/I_{NO_2}) as well as the dichroic ratio (R), order parameter (P_2), and average tilt angle (γ) obtained from polarization experiments.[a]

Peak assignment	Bulk [cm^{-1}]	LB [cm^{-1}]	I_X/I_{NO_2} Bulk	I_X/I_{NO_2} LB	$R_{ATR}=A_s/A_p$	P_2	γ [°]
$CH_{aromatic}$	3106, 3093	3096	0.03	0.08			
ν_a CH_3	2956	2959	0.10	0.39	1.13 ± 0.01	-0.01 ± 0.03	55
ν_a CH_2	2929	2928	0.12	0.41	1.06 ± 0.01	-0.16 ± 0.02	61
ν_s CH_2	2859	2856	0.06	0.23	1.03 ± 0.01	-0.21 ± 0.03	65
ν CN	2203	2205	0.27	0.09			
ν C=O	1735, 1718	1728	0.19	0.55	1.11 ± 0.00	-0.06 ± 0.00	57
ν $C=C_{ring}$	1601 (1579)[b]	(1607) 1591 (1577)	0.12	0.48	1.10 ± 0.02	-0.05 ± 0.03	57
ν_a NO_2	1534	1536	0.43	0.87	1.08 ± 0.01	-0.12 ± 0.02	60
ν C=C	1512	–	0.24				
δ_a CH_3	1456	1457	0.19	0.45	1.07 ± 0.01	-0.13 ± 0.03	60
ν C–O	1422	–	0.48				
	1403	–	0.44				
δ_s CH_3	1379	–	0.72				
ν_s NO_2	1336	1341	1.00	1.00	1.09 ± 0.01	-0.09 ± 0.03	58
ν COC	1281	(1288)	0.53	0.27			
ν COC	1255	(1262)	0.39	0.21			
ν COC	1235	(1242) (1222)	0.23	0.19			
ν_a COC	1207	–	0.31				
ν_a COC	1185	(1190)	0.53	0.18			
r_a CH_3	1151	1155	0.51	0.27			
r_a CH_3	1102	(1102)	0.19	0.16			
ν_s COC	1089	(1081)	0.15	0.15			
	1075	(1058)	0.11	0.13			
ν C–CH_3	1034	(1025)	0.14	0.11			

[a] See Experimental Section for details; [b] The position of peaks indicated in parentheses could be determined only approximately due to partial overlap with other peaks and/or low intensity.

chroic ratio (R_{ATR}) was calculated from the absorbance bands obtained with the infrared radiation polarized parallel (A_p) and perpendicular (A_s) to the plane of incidence. The associated order parameters with respect to the film normal (P_2) were then calculated by using mean-square electric field amplitudes obtained from the Harrick thin-film equations.[27] The values of R_{ATR}, P_2, and the average angle γ between the transition moment and the surface normal for the films transferred at the highest pressure ($25\,mN\,m^{-1}$) are given in Table 1 for the major bands. It is important to remember here that P_2 should be equal to zero for an isotropic sample ($\gamma=54.9°$, the magic angle), and to one and -0.5 for perfect orientation of the transition moments parallel ($\gamma=0°$) or perpendicular ($\gamma=90°$) to the surface normal, respectively. Table 1 shows that the order parameter differs significantly from zero for several bands. For example, a P_2 of about -0.2 is observed for the two methylene C–H stretching modes, revealing that the CH_2 groups are preferentially oriented in the plane of the LB film. Even though the high wavenumber position of the maximum of the 2859 and 2929 cm^{-1} bands shows that the alkyl chains are significantly disordered, as expected from the molecular model of the films (Figure 5), the polarized ATR results indicate that they are preferentially oriented along the surface normal with an average tilt angle of approximately 30°. On the other hand, the dichroic behavior of the 2960 cm^{-1} band indicates that the methyl groups are unoriented. The values for the γ angle of about 60° found for peaks corresponding to C=C and C=O double bonds and to the symmetric stretching vibration of the NO_2 groups at 1341 cm^{-1} (for which the transition moment is bissector of the NO_2 angle) shows unequivocally that the fluorene moiety is not lying flat on the surface, although a more precise determination

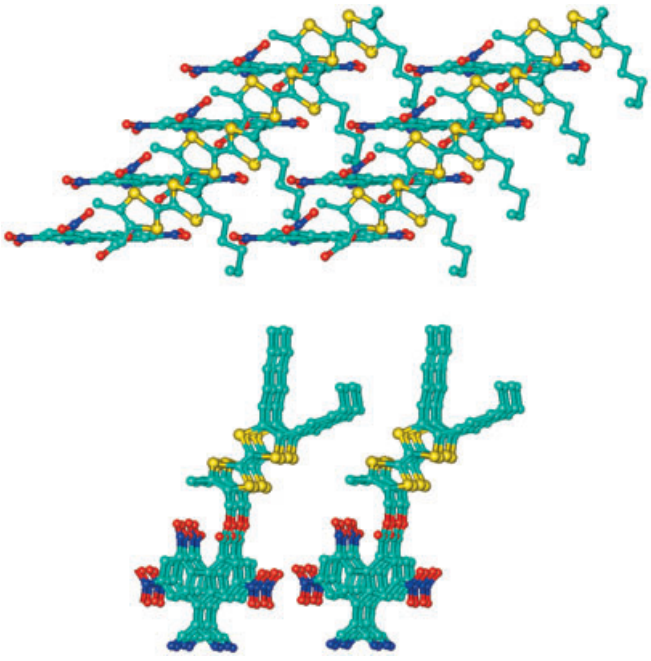

Figure 5. The top (above) and side (below) views of a model of an LB film of **8**, corresponding to a molecular area of 50 $Å^2$ (the TTF-fluorene core is the DFT optimized minimum energy conformer; the alkyl chains are added and optimized with the molecular mechanics force field MM+; the molecules are manually placed in the closest position, respecting van der Waals' distances; the hydrogen atoms are omitted for clarity).

of its orientation is precluded by the complexity of the structure (the presence of several similar bonds with different orientations). It is worth noting that reproducibility of the orientation measurements (presented by the absolute error in Table 1 calculated for three different films), while being quite acceptable for the films transferred at 25 mN m^{-1} was persistently very low for the films transferred at lower pressures (see the Supporting Information), as expected for poorly aligned low-density films.

Fabrication and electrical studies of n-Si/SiO_2/8/Ti junction devices: To investigate and verify the molecular rectification concept with **8**, we deposited a second electrode (10 nm Ti followed by 4 μm of Al) on top of the monolayers, transferred by X-type deposition on degeneratively n-doped Si wafers. The work functions of n-doped Si (4.85 eV) and Ti (4.33 eV) are similar to each other (to minimize the rectification of the p-n junction), and also fit reasonably well with the HOMO/LUMO levels of **8**.

The emerging picture of the deposition of metallic thin films, such as Ti and Au, on molecular monolayers is that the thickness and stoichiometry of the metallic film, as well as the structure of the molecular monolayer, all play critical roles in determining the extent to which the molecules are modified or damaged by the deposition.[28–31] Titanium is a unique metal for an evaporated top electrode. Due to its high reactivity, it immediately cleaves terminal C–H bonds forming a thin titanium carbide layer on the surface of the monolayer that may prevent further penetration of the Ti atoms inside the film,[29] as often observed for gold.[30–33] Preservation of the molecular features buried inside the aliphatic-chain-protected monolayers has been demonstrated by both X-ray photoelectron spectroscopy,[28] and more recently by RAIRS,[29] which showed disappearance of only terminal CH_3 vibrations, whereas all other infrared spectral features were unperturbed. In the same time, evaporation of a Ti layer of >30 Å on self-assembled monolayers (SAMs) of predictably more reactive conjugated compounds, such as oligothiophenes[31] or oligo(phenylethynylene)s,[30] can result in complete destruction of the molecules. SAMs are also lower density molecular monolayers than compressed LB films,[34] which would result in higher tilt angles and expose a larger part of the molecules to the incident Ti flux. In this paper, we have tried to account for these facts by putting protecting alkyl chains on the TTF moiety and by using highly compressed LB films.

We are also well aware of the criticism toward the claims of molecular rectification from junctions based on oxidizable metal contacts. The titanium oxide induced rectification was first pointed out by Ashwell et al. in 1980,[35] and a number of rectifying Ti-based junctions for molecules lacking an evident "diode" structure have been reported to date.[29,36] As was shown before,[35,36] such rectification depends upon the level of oxidation at the molecule/Ti interface and can be controlled by the level of vacuum used during the deposition of the Ti. Using a sufficiently high quality e-beam deposition system (providing a vacuum of 5×10^{-7} Torr), we are able to routinely control the vacuum, both to increase and to decrease the rectification. As shown below in control experiments, under the correct Ti deposition conditions, and for a degeneratively doped poly-Si bottom electrode, such rectification can be effectively suppressed and experimentally separated from the molecular features.

Current–voltage curves obtained for these devices are depicted in Figure 2 (bottom). We have earlier found for similar devices (LB monolayers sandwiched between poly-Si and Ti/Al electrodes) that the performance stabilizes if the devices are aged for several days prior to measurement,[21a] and such aging was done here. Notably, as the transfer pressure goes up, the magnitude of the current through the junction decreases, implying an increasing distance between the top and bottom electrodes as the monolayer aligns. The most dramatic effect, however, is that the rectification ratio (negative current/positive current, RR) sharply increases with increased transfer pressure, from 1.5 for 56 Å^2 per molecule to 5 for 52 Å^2 per molecule and 18 for 43 Å^2 per molecule. These observations are in agreement with the alignment of molecules of **8** during compression to form a well-packed monolayer with the D–A/surface angle being close to normal.

Note the only thing that changes for the devices in Figure 2 is the area per molecule, which translates into molecular orientation. Ellipsometric measurements of a film transferred at 17 mN m^{-1} (~50 Å^2 per molecule) suggested a thickness of 15–20 Å, consistent with the formation of a monolayer of the most stable conformer (shown in Figure 5). This conformer has a calculated thickness and molecular area of 21 Å and 50 Å^2, respectively. Further compression at pressures above ~17 mN m^{-1} would require conformational changes, and the film transferred at 25 mN m^{-2} most likely has both fluorene and TTF fragments perpendicular to the surface. Thus, any current–voltage asymmetry that might arise from the dissimilar electrodes, titanium oxide formation, and so forth is effectively a constant through this series of devices. Nevertheless, we checked this conclusion by preparing similar devices containing an eicosanoic acid LB monolayer in place of **8**. In a number of experiments performed, these devices yielded a RR of approximately 1.5–2, and never more than 3.[37] Furthermore, no dependence of the rectification ratio on the transfer pressure was found for eicosanoic acid, although the total current was also observed to decrease for films transferred at increasing values of area per molecule. Therefore, we assign the dominant contribution to the observed rectification in the monolayer of **8** as a molecular feature.

The maximum RR for an n-Si/**8**/Ti device is achieved at the relatively low potential of 0.9 V. Above 1.0 V, the rectification ratio decreases (see the Supporting Information). This is expected, because at sufficiently high applied bias, direct tunneling of charge carriers between the two electrodes becomes an increasingly important (and eventually dominant) mechanism of charge transport. In other words, at sufficiently high bias, the specific details of the molecule

become less important. The RR does not decrease (it actually slightly increases) after 10 scans (up to ± 1.75 V). This is in contrast to D-π-A systems in which the reorientation of highly polar molecules reduced the RR by a factor of two every second scan.[7b,8b] The direction of the observed rectification indicates that the preferred electron current is from the fluorene acceptor to the TTF donor (from Si on Ti).

Fabrication and electrical studies of Au/8/$C_{16}H_{32}$S-Hg junction devices: To investigate the effect of the electrode properties on the observed rectification we performed a similar study on the LB monolayer of **8** between higher-work-function gold and mercury electrodes (5.3 eV and 4.49 eV, respectively). The LB film of **8** was transferred onto a gold substrate in a previously described fashion (X deposition, Au/fluorene-σ-TTF interface), and the electrical junction was established by micromanipulator-controlled contacting with an octadecanethiol-protected hanging mercury drop electrode.[38] The dense defect-free Hg-$SC_{16}H_{33}$ monolayer prevents electrical shorts (due to possible defects in the LB layer) and formation of radical-ion salts on the mercury surface. Similar to Si/**8**/Ti devices, the I–V response of the Au/**8**/$C_{16}H_{32}$S-Hg junction is highly asymmetric (Figure 6) and

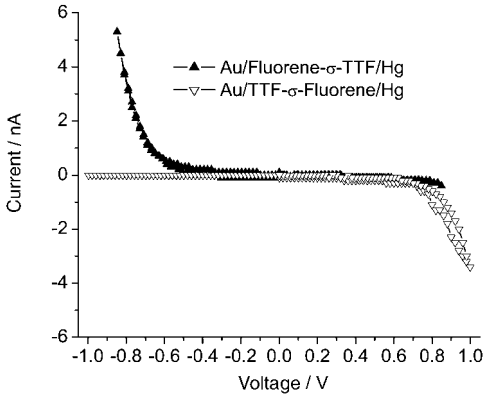

Figure 6. I-V characteristics of Au/**8**/$C_{16}H_{32}$S-Hg junction devices for different molecular orientations.

the RR ratio reached a value of 1:18 at 0.83 V (see the Supporting Information). The current densities achieved in these junctions are several orders of magnitude lower than those in Si/**8**/Ti devices, which is probably due to an additional insulating $C_{16}H_{33}S$ layer on the Hg electrode. Predictably, the stability of this junction device towards higher voltages and repeated voltage cycling is significantly lower than that of the Si/Ti device. The most important difference, however, was in the opposite rectification direction observed in this system (preferable electron flow in the TTF–fluorene direction, from Au to Hg). To exclude a possible rectification due to a Schottky barrier on the $C_{16}H_{33}S$-Hg interface,[39] we prepared a similar junction device with an opposite orientation of **8** on the gold surface (Z-type deposition).[40] As expected, the rectification direction changed the sign (electron flow from Hg to Au) to conform with the reversed TTF–fluorene orientation (Figure 6).

Although the exact mechanism of the different rectification directions in Si/Ti and Au/Hg junctions (A→D and D→A, respectively) is certainly disputable, we believe that the molecular origin of such behavior is adequately proved by the above molecular reorientation and alignment studies and control experiments with eicosanoic acid. A possible explanation could lie in the extremely low HOMO–LUMO gap of **8**, which in specific junction devices may change the ground state from a neutral TTF-σ-fluorene to a zwitterionic $TTF^{\bullet+}$-σ-$fluorene^{\bullet-}$ (in which the $TTF^{\bullet+}$ becomes an acceptor and $fluorene^{\bullet-}$ becomes a donor). Whatever the case, the results do highlight the important role that the electrodes play in determining the current–voltage response of a molecular electronic device.

Conclusion

To conclude, we have prepared and characterized the first molecular tunnel junctions based on a D-σ-A diad with an extremely low HOMO–LUMO gap (0.3 eV). The rectification behavior was found to increase rapidly to 1:18 upon alignment of the molecules in compressed Langmuir–Blodgett monolayers. An opposite rectification direction was found in n-Si/molecule/Ti and Au/molecule/Hg tunnel junctions, and the molecular origin of such behavior was confirmed by changing the orientation of the molecule (from D-σ-A to A-σ-D) and by control experiments with eicosanoic acid. Further studies including STM and conducting AFM characterization of the junctions are in progress.

Experimental Section

TTF–fluorene diad 8: This diad was obtained by an esterification reaction between substituted fluorene-4-carbonyl chloride and lithium TTF-methoxide, followed by condensation with malonodinitrile, as described earlier.[22]

Preparation of Langmuir–Blodgett (LB) films: Single monolayers were prepared at 20 °C on an aqueous (18.2 MOhm H_2O) subphase by using either a 600 cm^2 Nima 611D (Nima Technology, Coventry, UK) or a 400 cm^2 KSV 3000 (KSV Instruments, Helsinki, Finland) Langmuir–Blodgett (LB) trough. Images of the Langmuir films were recorded with a Nanofilm Surface Analysis Brewster angle microscope (BAM) (Göttingen, Germany). For compound **8**, a dilute buffer (5×10^{-4} M Na_2CO_3/$NaHCO_3$) was employed as a subphase in the trough to prevent acid-catalyzed oxidation of the TTF units. For the eicosanoic acid controls, a 3.045×10^{-4} M $CdCl_2$/6.415×10^{-5} M NaOH aqueous subphase was used. The molecules were first dissolved in slightly basic, freshly distilled chloroform (~0.5 g L^{-1}) and then immediately spread to the subphase to form the monolayer. After an equilibrating period of 30 min allowing solvent evaporation, the monolayer was compressed at constant speed of 10 mm min^{-1} and transferred at constant surface pressure onto the surface of interest (n-Si or Au electrodes for I–V experiments or Ge crystal for ATR experiments).

Characterization of 8 in monolayers: Contact angle and ellipsometry measurements for the monolayer were taken by depositing the monolayer on a bare Si ⟨111⟩ wafer and transferring at 17.0 mN m^{-1}. Contact angle measurements were obtained by using a Ramé Hart goniometer

100–00. Ellipsometry measurements were obtained using a Gaertner L116B Ellipsometer equipped with a He-Ne laser at 632.8 nm; a refractive index of 3.842 and an extinction coefficient of −0.016 were used for the silicon substrate. The refractive index of the monolayer was assumed to be 1.46 with an extinction coefficient of 0.00.

To perform ATR infrared measurements, single monolayers of **8** were transferred at a constant speed of 5 mm min^{-1} onto Ge parallelograms (angle of incidence 45°) of 50×20×2 mm, allowing 24 internal reflections. Before deposition, the substrates were cleaned with chloroform and methanol, immersed in chloroform in a Branson 1510 ultrasonic bath (Branson Ultrasonics Corporation, Danbury, CT) for 5 min, and put in a plasma cleaner (Harrick Scientific, Ossining, NY) for 2 min. Finally, dust was removed with a nitrogen gas flow. The germanium crystals were placed in a vertical ATR accessory (Harrick Scientific, Ossining, NY) and the spectra were recorded using Magna 550 FTIR spectrometer (Thermo-Nicolet, Madison, WI) equipped with a liquid-N_2 cooled MCT detector. A motorized rotating ZnSe wire-grid polarizer (Specac, Orpington, UK) was positioned in front of the sample to obtain parallel- and perpendicular-polarized spectra without breaking the purge of the spectrometer. A total of 500 scans at 4 cm^{-1} was sufficient to achieve a high signal-to-noise ratio. RAIRS spectroscopy was performed for monolayers of **8** transferred onto gold substrates by using a Nexus 670 FTIR spectrometer (Thermo-Nicolet, Madison, WI) equipped with a liquid-N_2 cooled MCT-II detector and grazing angle (80°) Smart-SAGA accessory. The measurements were done in an atmosphere of dried, CO_2-free air, and an identical gold-covered slide (prepared in the same Au-evaporation run), freshly cleaned by soaking in HPLC-grade dichloromethane and drying in vacuo, was used to record a background spectrum.

Fabrication and studies of Si/8/Ti junctions: The process for the fabrication of the solid-state molecular diode tunnel junctions follows the methods described previously.[21] For the bottom electrodes, a layer of n-type polycrystalline (poly-Si) was formed by means of direct chemical vapor deposition growth onto ⟨100⟩ Si wafers coated with oxide. The poly-Si was then etched into 5 μm wide electrodes by using standard optical lithography techniques. The LB monolayer of **8** was transferred onto the silicon substrate by X-type deposition (the substrate was lifted up from the subphase). A top electrode of 10 Å titanium, followed by 4000 Å aluminum, was then deposited on top of the monolayer by electron-beam evaporation at a residual pressure of ~5×10^{-7} Torr.

Current–voltage characteristics were taken in air at room temperature by using a shielded probe station with coaxial probes. For Si/**8**/Ti junctions, bias voltages were applied to the polysilicon electrode, and the top metal electrode was connected to ground through a Stanford Research Systems SR570 low-noise current preamplifier.

Fabrication and studies of Au/8/$C_{16}H_{33}$S-Hg junctions: The junction was assembled in a procedure, similar to the described before.[36] A gold layer (~200 nm) was thermally evaporated on ⟨100⟩ Si wafers or freshly cleaved mica slides. Before the LB film transfer, the gold surface was cleaned by 10 min exposure to O_2-plasma followed by immersing in HPLC grade ethanol to decompose the formed oxides.[41] The LB film of **8** was transferred (always at 25 mN m^{-1}) on thus prepared substrate in X or Z deposition mode, resulting in formation of Au/fluorene-σ-TTF or Au/TTF-σ-fluorene sandwiches, respectively. The gold substrate was put under deionized water (to improve the stability of the junction; ion-exchange purification followed by distillation was employed to reduce the water conductivity, whereas no other solvent could be used due to LB film instability). A hanging drop of mercury (from a microsyringe, ~500 μm in diameter), covered with a monolayer of octadecylthiolate by 15 min exposure to a solution of $C_{16}H_{33}SH$ in ethanol and rinsed with fresh ethanol, was brought into contact with the monolayer of **8** under the water, by using a micromanipulator. The substrate was grounded, the bias voltages were applied to the mercury electrode (two-electrode scheme), and the I-V characteristics were recorded with a potentiostat EG&G PAR273 A (sensitivity 0.1 nA) at a scan rate of 1000 mV s^{-1} and sampling rate of 20 mV per point. The voltage and current polarity in Figure 6, however, are reversed for consistency with the Si/Ti junction data, for which an opposite polarity scheme was used.

Calculations: The geometry optimization was performed at the DFT (RB3LYP) level of theory, by using the 6–31G(d) basis set, as implemented in Gaussian 98.[42] The calculated RB3LYP wavefunction was found to be stable according to the Gaussian stability test. The frequency check for all conformations was used to confirm that they are true minima.

Acknowledgements

This work was supported by the Defense Advanced Research Projects Agency and by the MARCO focus center on Advanced Materials and Devices (in USA), NSERC and FQRNT grants (in Canada) and EPSRC (in UK).

[1] J. Ferraris, D. O. Cowan, V. V. Walatka, J. H. Perlstein, *J. Am. Chem. Soc.* **1973**, *95*, 948–949.
[2] A. Aviram, M. A. Ratner, *Chem. Phys. Lett.* **1974**, *29*, 277–283.
[3] R. M. Metzger, *Chem. Rev.* **2003**, *103*, 3803–3834.
[4] R. L. Carroll, C. B. Gorman, *Angew. Chem.* **2002**, *114*, 4556–4579; *Angew. Chem. Int. Ed.* **2002**, *41*, 4378–4400.
[5] G. Maruccio, R. Cingolani, R. Rinaldi, *J. Mater. Chem.* **2004**, *14*, 542–554.
[6] a) G. J. Ashwell, J. R. Sambles, A. S. Martin, W. G. Parker, *J. Chem. Soc. Chem. Commun.* **1990**, 1374–1376; b) A. S. Martin, J. R. Sambles, G. J. Ashwell, *Phys. Rev. Lett.* **1993**, *70*, 218–221.
[7] a) R. M. Metzger, B. Chen, U. Höpfner, M. V. Lakshmikantham, D. Vuillaume, T. Kawai, X. Wu, H. Tachibana, T. V. Hughes, H. Sakurai, J. W. Baldwin, C. Hosch, M. P. Cava, L. Brehmer, G. J. Ashwell, *J. Am. Chem. Soc.* **1997**, *119*, 10455–10466; b) R. M. Metzger, *Acc. Chem. Res.* **1999**, *32*, 950–957; c) R. Xu, I. R. Peterson, M. V. Lakshmikantham, R. M. Metzger, *Angew. Chem.* **2001**, *113*, 1799–1802; *Angew. Chem. Int. Ed.* **2001**, *40*, 1749–1752; d) R. M. Metzger, T. Xu, I. R. Peterson, *J. Phys. Chem. B* **2001**, *105*, 7280–7290.
[8] a) G. J. Ashwell, R. Hamilton, L. R. H. High, *J. Mater. Chem.* **2003**, *13*, 1501–1503; b) G. J. Ashwell, A. Chwialkowska, L. R. H. High, *J. Mater. Chem.* **2004**, *14*, 2389–2394.
[9] a) G. J. Ashwell, D. S. Gandolfo, *J. Mater. Chem.* **2001**, *11*, 246–248; b) G. J. Ashwell, D. S. Gandolfo, *J. Mater. Chem.* **2002**, *12*, 411–415; c) G. J. Ashwell, D. S. Gandolfo, R. Hamilton, *J. Mater. Chem.* **2002**, *12*, 416–420; d) G. J. Ashwell, W. D. Tyrrell, A. J. Whittam, *J. Am. Chem. Soc.* **2004**, *126*, 7102–7110.
[10] a) J. Chen, M. A. Reed, A. M. Rawlett, J. M. Tour, *Science* **1999**, *286*, 1550–1552; b) more recent results suggest that formation and dissolution of metal monofilaments may be primarily responsible for the negative differential resistance observed in reference [10a]: J. M. Tour, L. Cheng, D. P. Nackashi, Y. Yao, A. K. Flatt, S. K. St. Angelo, T. E. Mallouk, P. D. Franzon, *J. Am. Chem. Soc.* **2003**, *125*, 13279–13283.
[11] a) M.-K. Ng, L. Yu, *Angew. Chem.* **2002**, *114*, 3750–3753; *Angew. Chem. Int. Ed.* **2002**, *41*, 3598–3601; b) P. Yiang, G. M. Morales, W. You, L. Yu, *Angew. Chem.* **2004**, *116*, 4571–4575; *Angew. Chem. Int. Ed.* **2004**, *43*, 4471–4475.
[12] F. C. Krebs, H. Spanggaard, N. Rozlosnik, N. B. Larsen, M. Jørgensen, *Langmuir* **2003**, *19*, 7873–7880.
[13] M. Pomerantz, A. Aviram, R. A. McCorkle, L. Li, A. G. Schrott, *Science* **1992**, *255*, 1115–1118.
[14] C. Zhou, M. R. Deshpande, M. A. Reed, L. Jones II, J. M. Tour, *Appl. Phys. Lett.* **1997**, *71*, 611–613.
[15] J.-O. Lee, G. Lientschnig, F. Wiertz, M. Struijk, R. A. J. Janssen, R. Egberink, D. N. Reinhoudt, P. Hadley, C. Dekker, *Nano Lett.* **2003**, *3*, 113–117.
[16] M. L. Chabinyc, X. Chen, R. E. Holmin, H. Jacobs, H. Skulason, C. D. Frisbie, M. V. Mujica, M. A. Ratner, M. A. Rampi, G. M. Whitesides, *J. Am. Chem. Soc.* **2002**, *124*, 11730–11736.
[17] S. Lenfant, C. Krzeminski, C. Delerue, G. Allan, D. Vuillaume, *Nano Lett.* **2003**, *3*, 741–746.

[18] J. Taylor, M. Brandbyge, K. Stokbro, *Phys. Rev. Lett.* **2002**, *89*, 138301.
[19] a) N. J. Geddes, J. R. Sambles, D. J. Jarvis, W. G. Parker, *Appl. Phys. Lett.* **1990**, *56*, 1916–1918; b) A. C. Brady, B. Hodder, A. S. Martin, J. R. Sambles, C. P. Ewels, R. Jones, P. R. Briddon, A. M. Musa, C. A. Panetta, *J. Mater. Chem.* **1999**, *9*, 2271–2275; c) R. M. Metzger, J. W. Baldwin, W. J. Shumate, I. R. Peterson, P. Mani, G. J. Mankey, T. Morris, G. Szulczewski, S. Bosi, M. Prato, A. Comito, Y. Rubin, *J. Phys. Chem. B* **2003**, *107*, 1021–1027.
[20] K. Stokbro, J. Taylor, M. Brandbyge, *J. Am. Chem. Soc.* **2003**, *125*, 3674–3675.
[21] a) C. P. Collier, G. Mattersteig, E. W. Wong, Y. Luo, K. Beverly, J. Sampaio, F. M. Raymo, J. F. Stoddart, J. R. Heath, *Science* **2000**, *289*, 1172–1175; b) C. P. Collier, J. O. Jeppesen, Y. Luo, J. Perkins, E. W. Wong, J. R. Heath, J. F. Stoddart, *J. Am. Chem. Soc.* **2001**, *123*, 12632–12641.
[22] a) D. F. Perepichka, M. R. Bryce, A. S. Batsanov, E. J. L. McInnes, J. P. Zhao, R. D. Farley, *Chem. Eur. J.* **2002**, *8*, 4656–4669; b) D .F. Perepichka, M. R. Bryce, E. J. L. McInnes, J. P. Zhao, *Org. Lett.* **2001**, *3*, 1431–1434.
[23] a) W. Koch, M. C. Holthausen, *A Chemist's Guide to Density Functional Theory*, Wiley-VCH, **2000**; b) O. V. Baerends, O. V. Gritsenko, *J. Phys. Chem. A* **1997**, *101*, 5383–5403.
[24] D. F. Perepichka, M. R. Bryce, C. Pearson, M. C. Petty, E. J. L. McInnes, J. P. Zhao, *Angew. Chem.* **2003**, *115*, 4783–4787; *Angew. Chem. Int. Ed.* **2003**, *42*, 4635–4639.
[25] H. Ishii, K. Sugiyama, E. Ito, K. Seki, *Adv. Mater.* **1999**, *11*, 605–625.
[26] M. V. Lakshmikantham, A. F. Garito, M. P. Cava, *J. Org. Chem.* **1978**, *43*, 4394–4395.
[27] F. Picard, T. Buffeteau, B. Desbat, M. Auger, M. Pézolet, *Biophys. J.* **1999**, *76*, 539–551.
[28] K. Konstadinidis, P. Zhang, R. L. Opila, D. L. Allara, *Surf. Sci.* **1995**, *338*, 300–312.
[29] S. C. Chang, Z. Li, C. N. Lau, B. Larade, R. S. Williams, *Appl. Phys. Lett.* **2003**, *83*, 3198–3200.
[30] A. V. Walker, T. B. Tighe, J. Stapleton, B. C. Haynie, S. Upilli, D. L. Allara, N. Winograd, *Appl. Phys. Lett.* **2004**, *84*, 4008–4010.
[31] B. de Boer, M. F. Frank, Y. J. Chabal, W. Jiang, E. Garfunkel, Z. Bao, *Langmuir* **2004**, *20*, 1539–1542.
[32] G. Philipp, C. Müller-Schwanneke, M. Burghard, S. Roth, K. v. Klitzing, *J. Appl. Phys.* **1999**, *85*, 3374–3376.
[33] A. V. Walker, T. B. Tighe, O. M. Cabarcos, M. D. Reinard, B. C. Haynie, S. Uppili, N. Winograd, D. L. Allara, *J. Am. Chem. Soc.* **2004**, *126*, 3954–3963.
[34] Comparisons of area per molecule values for monolayers of two very similar [2]rotaxane molecules showed the molecular area of >300 Å^2 per molecule for SAM and only <140 Å^2 per molecule for LB films: a) H.-R. Tseng, D. Wu, N. X. Fang, X. Zhang, J. F. Stoddart, *ChemPhysChem* **2004**, *5*, 111–116; b) Y. Luo, C. P. Collier, J. O. Jeppesen, K. A. Nielsen, E. DeIonno, G. Ho, J. Perkins, H.-R. Tseng, T. Yamamoto, J. F. Stoddart, J. R. Heath, *ChemPhysChem* **2002**, *3*, 519–525.
[35] G. J. Ashwell, J. S. Bonham and L. E. Lyons, *Aust. J. Chem.* **1980**, *33*, 1619–1623.
[36] a) R. McCreery, J. Dieringer, A. O. Solak, B. Snyder, A. M. Nowak, W. R. McGovern, S. DuVall, *J. Am. Chem. Soc.* **2003**, *125*, 10748–10758; b) R. McCreery, J. Dieringer, A. O. Solak, B. Snyder, A. M. Nowak, W. R. McGovern, S. DuVall, *J. Am. Chem. Soc.* **2004**, *126*, 6200. Molecular rectification was claimed for azobenzene derivative contacted with Ti electrode in reference [36a], but was retracted in reference [36b], showing symmetric I–V characteristics when fabricated in an oxygen-free environment.
[37] An increased rectification ratio (and lower absolute currents), consistent with formation of titanium oxide layer, can be observed for eicosanoic acid junctions when fabricated at higher residual pressure ($\geq 10^{-5}$ Torr), see references [35,36].
[38] a) R. Haag, M. A. Rampi, R .E. Holmlin, G. M. Whitesides, *J. Am. Chem. Soc.* **1999**, *121*, 7895–7906; b) R. E. Holmlin, R. Haag, M. L. Chabinyc, R. F. Ismagilov, A .E. Cohen, A. Terfort, M. A. Rampi, G. M. Whitesides, *J. Am. Chem. Soc.* **2001**, *123*, 5075–5085.
[39] A weak rectification (RR ~ 1:2) was recently demonstrated for a molecular junction device fabricated with octadecanethiol sandwiched between two gold electrodes and covalently bound to only one electrode: M. D. Austin, S. Y. Chou, *Nano Lett.* **2003**, *3*, 1687–1690.
[40] Unfortunately, a similar experiment with reversed molecular orientation is not possible for Si/**8**/Ti junctions, because the reactive fluorene acceptor fragment lacks the protecting alkyl tail and cannot be exposed to Ti.
[41] H. Ron, S. Matlis, I. Rubinstein, *Langmuir* **1998**, *14*, 1116–1121.
[42] Gaussian 98, Revision 5.4, M. J. Frisch, G. W. Trucks, H. B. Schlegel, G. E. Scuseria, M. A. Robb, J. R. Cheeseman, V. G. Zakrzewski, J. A. Montgomery, R. E. Stratmann, J. C. Burant, S. Dapprich, J. M. Millam, A. D. Daniels, K. N. Kudin, M. C. Strain, O. Farkas, J. Tomasi, V. Barone, M. Cossi, R. Cammi, B. Mennucci, C. Pomelli, C. Adamo, S. Clifford, J. Ochterski, G. A. Petersson, P. Y. Ayala, Q. Cui, K. Morokuma, D. K. Malick, A. D. Rabuck, K. Raghavachari, J. B. Foresman, J. Cioslowski, J. V. Ortiz, B. B. Stefanov, G. Liu, A. Liashenko, P. Piskorz, I. Komaromi, R. Gomperts, R. L. Martin, D. J. Fox, T. Keith, M. A. Al-Laham, C. Y. Peng, A. Nanayakkara, C. Gonzalez, M. Challacombe, P. M. W. Gill, B. G. Johnson, W. Chen, M. W. Wong, J. L. Andres, M. Head-Gordon, E. S. Replogle, J. A. Pople, Gaussian, Pittsburgh, PA, **1998**.

Received: November 5, 2004
Published online: February 18, 2005